Research Article Received: 2024-03-18, Accepted: 2024-04-12

Voltammetry of Constant Phase Elements: Analyzing Scan Rate Effects

*Hyeonsu Je, Byoung-Yong Chang**

Department of Chemistry, Pukyong National University, 45 Yongso-ro, Nam-gu, Busan 608-739, Korea;

Email: bychang@pknu.ac.kr; phone: +82-51-629-5597; fax: +82-51-629-5583

ABSTRACT

Here we introduce a new method for characterizing the constant phase element (CPE) in electrochemical systems using cyclic voltammetry (CV), presenting an alternative to the conventional electrochemical impedance spectroscopy (EIS) approach. While CV is recognized for its diagnostic capabilities in electrochemical analysis, it traditionally encounters difficulties in accurately measuring CPE systems due to a lack of clear linearity with scan rates, unlike capacitors. Our research demonstrates a linear relationship between current and scan rate on a log-log plot, enabling the calculation of n and Y_0 values for CPE from the slopes of these linear relationships. For validation of our method, it is applied to two kinds of capacitors and the results agree with those measured by EIS. Although EIS is known to be accurate in measuring CPE systems, our alternative approach offers a

DOI: 10.33961/jecst.2024.00318

timely and reasonably precise diagnostic tool, balancing between ease of use and accuracy, especially beneficial for preliminary assessments before conducting further in-depth analysis.

Keywords: cyclic voltammogram, constant phase element, electrochemical impedance

Introduction

Voltammetry stands out as the most recognized electrochemical technique due to its versatility and sensitivity[1, 2], providing in-depth insights into electrochemical dynamics through current measurement as potential varies. This technique is particularly useful for examining faradaic processes, including redox reactions[3] and kinetics of charge and mass transfers[4, 5], which are essential for advancement of analysis [6, 7], energy storage systems[8] and so on. Moreover, voltammetry provides the foundational knowledge required to study non-faradaic processes, including capacitive behavior[9] and interactions at the electrode surface[10], which are vital for material characterization and supercapacitor research[11].

While voltammetry provides invaluable insights for electrochemical research, it encounters limitations in accurately measuring the electric double layer, largely due to non-ideal capacitive behaviors. These issues are primarily observed at the interface between solid electrodes and liquid electrolytes[12], making the analysis of capacitive properties more complex. On the other hand, electrochemical impedance spectroscopy (EIS) offers more precise measurements in the frequency domain, attributing these discrepancies to phase shifts not equal to 90 degrees and introducing the concept of a constant phase element (CPE) to explain them[13, 14]. The CPE, characterized by its unique phase and frequency-dependent attributes, reveals intricate electrochemical processes not evident in other fields, underscoring the complexity and richness of studying electrochemical interfaces[15, 16].

While EIS is believed to be superior for CPE measurement[17], offering in-depth analysis of the electric double layer's non-ideal behavior through extensive frequency domain experiments, voltammetry may be better in its diagnostic capabilities through swift time domain analysis[18]. Despite not directly measuring CPE properties as effectively as EIS, voltammetry's advantages lie in its rapidity and simplicity, rendering it suitable for quick diagnostics and high-throughput applications. Furthermore, it facilitates direct comparisons of current and potential, offering clear insights into electrochemical reactions in straightforward way. Therefore, enhancing voltammetry techniques for better assessment of the electric double layer and interpretation of CPEs are pursued, positioning voltammetry as a complementary approach to EIS[19] in electrochemical research.

Even though the CPE is frequently used to analyze electrochemical systems in the frequency domain, especially for calculating the effective capacitance of non-ideal capacitive processes, its application in the time domain is less common. Sadkowski et al. employed fractional calculus and numerical methods to model the time-domain responses of a CPE in cyclic voltammetry (CV) and corrosion systems, remarking the lack of analytical solutions for potential sweeps[20]. Sagüés utilized a finite difference numerical method to analyze non-ideal capacitive behavior modeled by a CPE responding to linear potential in the time domain[21]. Feliu et al. developed a computational algorithm using numerical simulation and a discretized approximation of a fractional derivative operator to evaluate the transient current of a CPE[22]. Recently, time-domain analysis of CPE has shifted its focus from corrosion research to evaluating the effective capacitance of CPE using voltammetry. J. P. Zheng et al. measured voltammetric currents of ionic liquid-based capacitors to obtain capacitance, observing

discrepancies from the theoretical linear relationship between current and scan rate[23]. In their subsequent reports, they employed EIS to accurately measure capacitance using the CPE model, then compared these findings with voltammetry and impedance spectroscopy results[24]. A. Allagui et al. highlighted conventional voltammetry's limitations in precisely evaluating CPE capacitance in electric double-layer capacitors and introduced equations that describe the voltammetric current by solving fractional differential equations[25]. P. Charoen-amornkitt et al. advanced mathematics similarly to elucidate voltammetric current, incorporating charge and mass transfers as well as CPE effects[26-28]. Conversely, C. Yun et al. obtained a voltammogram by applying an inverse Fourier transform to the impedance spectra from an equivalent circuit containing a CPE, aiding in understanding charging and discharging processes[29]. M. Schalenbach et al. also utilized this method to generate voltammograms for investigating the dynamic distortion during electric double layer charging[30]. S. M. Gateman et al., in their review[31], compared CPE analyses by EIS and cyclic voltammetry (CV), concluding that EIS yields more accurate results and cautioning against using a pure capacitor model in place of a CPE in CV studies.

In prior research above, formulas for analyzing voltammograms were developed[25, 27], allowing for the extraction of information about the CPE through regression analysis of measured data. Yet, when the benefits of voltammetry are taken into account, data analysis based on computational regression may not be the unique advantage that we expect from voltammetry. One of the strengths of voltammetry is the ability to linearly relate current, potential, and time, which can elucidate various electrochemical phenomena. For example, the relationship between peak current and the square root

of the scan rate can reveal details about faradaic reactions, while a direct correlation between current and scan rate can provide information on the electric double layer. Such linear relationships provide critical information in a clear and accessible manner. Nevertheless, the characterization of the CPE using voltammetry faces significant challenges, primarily due to the non-linear behavior observed with varying scan rates. Previous studies have attempted to characterize the CPE based on scan rate[32]; however, the non-linearity complicates straightforward evaluation. Scheme 1 illustrates this issue by comparing the currents of a pure capacitor and a CPE as the scan rate increases. Unlike the linear increase observed with the pure capacitor (black line), the CPE exhibits a non-linear rise (red line), hindering the direct application of capacitive properties to the CPE. The dashed blue lines in the graph indicate how linearity changes with varying scan rates. This non-linearity obstructs the clear advantages voltammetry offers, suggesting a need for refined methodologies that can accommodate the unique behaviors of the CPE.

This study intends to extend this groundwork by examining the linearity of CPE voltammograms concerning scan rates, proposing a voltammetry-based method for CPE characterization. Being complementary to EIS, this method exploits the diagnostic power of voltammetry to enhance our understanding of CPE and its capacitive behavior, thus advancing electrochemical system analysis.

Theory

A CPE is characterized by two parameters: Y_0 and n. Y_0 denotes a specific property intrinsic to the CPE, while n represents the phase shift, quantified as $n\pi/2$ Typically, the impedance of a CPE is denoted as Z_{CPE} and described by the following equation:

$$Z_{\mathrm{CPE}} = \frac{1}{(j\omega)^n Y_0} \quad \text{eq (1)}$$

Based on eq (1), the current in the frequency domain, $I(s)$, is formulated as[20]:

$$I(s) = Y_0 \frac{d^n E(s)}{ds^n} \quad \text{eq (2)}$$

Upon sweeping the potential at a scan rate of v, and corresponding to $E(t) = E_0 + vt$, the current in the time domain, $i(t)$, can be calculated by solving the fractional differential equation[25]. However, due to the absence of a direct solution for obtaining a closed-form equation, $i(t)$ can be approximately derived under the boundary condition that E_0 is the potential of zero current.

$$i(t) = Y_0 \frac{E(t)-E_0}{t} \frac{t^{1-n}}{\Gamma(2-n)} \quad \text{eq (3)}$$

With $E(t) = E_0 + vt$, we can transform this equation to describe the voltammetric current as follows:

$$i(E) = Y_0 v \frac{(E-E_0/v)^{1-n}}{\Gamma(2-n)} = Y_0 \frac{(E-E_0)^{1-n}}{\Gamma(2-n)} v^n \quad \text{eq (4)}$$

This equation demonstrates that the current is contingent upon the scan rate, exhibiting a specific linear relationship with v^n. By reorganizing this equation in logarithmic form:

$$\log i(E) = \log Y_0 \frac{1}{\Gamma(2-n)} (E - E_0)^{1-n} + n \log v \quad \text{eq(5)}$$

It elucidates a linear correlation between the current and the scan rate. By plotting a log-log plot for the current against the the scan rate, we can determine of n and Y_0, the characteristic parameters of the CPE, from the slope and intercept, respectively.

Experimental

Computational simulation

The computational simulation of cyclic voltammograms for a circuit comprising a constant phase element (CPE) and a resistor was conducted using the inverse Fourier transform method. As this method is comprehensively described in the prior studies[29, 30], here we only briefly outline the methodological approach employed.

The applied potential, as a function of time, is modeled with a triangular waveform. However, this waveform can alternatively be expressed in terms of frequency (ω) as the sum of AC waves at harmonic frequencies. The mathematical representation of this concept is given by:

$$E(t) = \frac{8}{\pi^2}\sum_{m=1,3,5}^{M}\frac{(-1)^{(m-1)/2}}{m^2}sin(m\omega t) \qquad \text{eq (6)}$$

This equation enables the determination of the amplitude of individual AC waves at frequency ω, denoted as $E(\omega)$. These amplitudes are used for calculating the current response, $i(\omega)$ of an equivalent circuit modelling an electrochemical system. Following the calculation of $i(\omega)$, an inverse Fourier transform is applied to convert $i(\omega)$ back into the time domain, resulting in $i_\omega(t)$. By summing up the individual current responses, we obtain the overall current $i(t)$ which finally constructs a voltammogram when it plotted vs. $E(t)$ in eq (6).

Electrochemical experiment

A simple polyaniline pseudo-capacitor was assembled by integrating two polyaniline electrodes with a cellulose paper-based electrolyte layer. The polyaniline electrodes were fabricated through the electrochemical deposition process on indium tin oxide (ITO)-coated glass substrates. This process utilized a potential sweep from -0.2 V to 1.2 V versus an Ag|AgCl reference electrode at a scan rate of 100 mV/s, in an electrolytic solution containing 30 mM aniline and 0.50 M H_2SO_4[33]. The electrolyte layer was prepared by immersing cellulose paper (Kimwipes, obtained from Kimtech) in a 0.50 M H_2SO_4 solution to ensure ionic conductivity between the electrodes. A commercial supercapacitor, model BCAP0005, was purchased from Maxwell Technologies Korea Co., Ltd. It's rated capacitance is 5 F, with performance specifications indicating a range from a minimum of 4.5 F to a maximum of 6.0 F depending on the applied voltage. All electrochemical analyses were conducted employing an SP-200 (Biologic, France), a potentiostat equipped with an AC module capable of electrochemical impedance spectroscopy.

Results and discussions

Figure 1 illustrates the theoretical appearance of a CPE system's voltammogram across different *n* values. When *n* equals 1, the CPE behaves as an ideal capacitor, exhibiting the expected rectangular shape in the cyclic voltammogram. Deviation from $n = 1$ leads to increasing distortion of the voltammogram, moving away from its characteristic capacitive behavior. This observation is consistent with findings reported in the literature, further validating the accuracy of our computer simulations.

Determination of n of the CPE

Figure 2 presents cyclic voltammograms of a CPE with n = 0.8 simulated at various scan rates, showing that, similar to an ideal capacitor, the CPE's voltammetric current increases with scan rates. However, unlike a capacitor or a CPE with n = 1, where current rises linearly with scan rate, a CPE with $n \neq 1$ exhibits a non-linear current increase with scan rate (v). To utilize eq (5), the log of current is plotted against log v, with currents sampled at E = 0.4, 1.0, and 1.6 V as shown in Figure 3, revealing a consistent linear relationship. This analysis indicates an n value of 0.8, which remains constant across different potentials, while intercept values vary with potential, aligning with the expectations of eq (5). Subsequently, currents are plotted against v^n, revealing that current linearly increases with v raised to the power of n, as depicted in Figure 4. This linearity is general including special cases; for n = 1, the CPE is a capacitor and current increases linearly with scan rate, and for n = 0.5, the CPE is the Warburg impedance controlled by diffusion, the increase of current with $v^{1/2}$ is the same as diffusion-limited current increasing with $v^{1/2}$.

Estimation of Y_0 of the CPE

Given the linear relationship between current and v^n, the value of Y_0 is deducible from the slope, expressed as $Y_0 \frac{1}{\Gamma(2-n)}(E - E_0)^{1-n}$. It is important to recognize that the slope represents not only Y_0 but is also influenced by the applied potential, necessitating careful consideration during its calculation. Figure 4 illustrates how the slopes of the fitting curves vary with the potential used to measure the

current, showing steeper slopes at higher potentials as predicted by eq (4). Yet, applying this equation for slope calculation is problematic because the derivation of eq (4) assumes a steady-state condition for CPE charging[25]. However, during the initial phase of current flow through the CPE, these steady-state conditions are not met and E_0 has no certain value to solidify eq (4). Figure 5 visually highlights the deviation of the voltammogram predicted by eq (4) from that generated through computational simulation, effectively illustrating that the currents anticipated by the equation do not align with the expected steady-state conditions.

Rather than determining the precise value of Y_0 through rigorous calculation as detailed in the prior studies, we propose estimating Y_0 within an acceptable margin of error using voltammetry. Given the practical uncertainties of achieving the steady-state condition required for $\frac{1}{\Gamma(2-n)}(E-E_0)^{1-n}$, it is advisable to substitute this term with experimental parameters that are indicative of potential. As depicted in Figure 5, the terminal potentials appear to fulfill this criterion, allowing for the assignment of a practical value to $(\Delta E)^{1-n}$ where ΔE represents the potential range of the cyclic voltammogram and the current, $i(t)$, is measured at the end potential. The adaptation of the variable E can be approximately achieved through a specific correction factor:

$$\frac{1}{\Gamma(2-n)}(E-E_0)^{1-n} \cong \frac{a}{\Gamma(2-n)}(\Delta E)^{1-n} \quad \text{eq(7)}$$

In this formula, the correction factor is represented by a, which depends on n and ΔE. P. Charoen-Amornkitt et. al conducted numerical simulations to determine the values of a with varying n and ΔE, documenting each corresponding value in their report[27]. Notably, when the potential window is

sufficiently wide, the correction factor approaches $\Gamma(2-n)$. Substituting eq (7) into eq (4) results in a revised formulation of Y_0, as presented in Equation (8):

$$Y_0 = \frac{Slope}{(\Delta E)^{1-n}} \quad \text{eq (8)}$$

This alternative approach facilitates the calculation of Y_0 values under various experimental conditions. To validate eq (8), cyclic voltammograms are obtained through digital simulation, adjusting n from 0.7 to 1.0 and ΔE from 0.5 to 4.0 V. The n values are calculated using Equation (5), followed by the computation of Y_0 values using Equation (8). These calculated Y_0 values are then compared to the actual values, with the discrepancies presented as percentages in Table 1. Although these are approximated values with permissible error margins, the variances are minor enough to be considered acceptable to validate the use of voltammetry as an effective and expedient diagnostic technique.

Applications to pseudo-capacitors

A methodology has been developed to determine the parameters n and Y_0 of the of the constant phase element (CPE) through cyclic voltammetry, and its applications are demonstrated to practical electrochemical systems.

Polyaniline, a common material for fabricating pseudo-capacitors, accumulates charge through faradaic reactions when coated on an electrode. Unlike traditional capacitors, which store charge by non-faradaic process and described as capacitor, polyaniline behaves similarly but is more accurately described by a CPE model because its charge storage mechanism involves faradaic processes. Figure

6 presents cyclic voltammograms of a polyaniline pseudo-capacitor at varying scan rates, with measurements taken at E = 0.5 V. Plotting log(current) against log v unveils a linear relationship. Linear regression of these data points provides n = 0.72, characterizing the pseudo-capacitor's CPE behavior.

Figure 7 illustrates the relationship between current and both v and v^n. Here, the current scales linearly with v^n in (b), deviating from the expected behavior for a conventional capacitor, which would exhibit linearity with v in (a). This key observation supports modeling the electrochemical cell as a CPE rather than a traditional capacitor. Using the determined slope and potential range, Y_0 is estimated to be 0.18 $S \cdot s^n$. To validate these findings, we conducted electrochemical impedance spectroscopy, with the resultant Nyquist plot displayed in Figure 8. The data were fit to an equivalent circuit model consisting of a CPE connected to a serial and a parallel resistors[17], confirming the calculated CPE values of n = 0.71 and Y_0 = 0.18 $S \cdot s^n$.

A commercial super-capacitor with a specific capacitance of 5 F is investigated by cyclic voltammetry. Figure 9(a) displays the cyclic voltammograms obtained at various scan rates. Given that these voltammograms do not exhibit the ideal rectangular shape typically associated with capacitive behavior, the electrochemical cell is more accurately modeled as a CPE. For CPE characterization, we plotted log(current) against log v, from which the slope indicates an n value of 0.98 (data not shown). Subsequently, currents are measured at E = 1.5 V and plotted against v^n, as illustrated in part (b) to demonstrate a clear linear relationship.

According to Equation (7), the value of Y_0 is calculated to be 4.47 S·s^n. Given that the n value is nearly unity, this indicates that Y_0 can be effectively considered as the capacitance of the system. Thus, the determined value of 4.47 S·s^n closely approximates the supercapacitor's specified minimum capacitance of 4.5 F at low operation voltages, confirming the validity of the model in describing the electrochemical behavior of the device.

Conclusion

Voltammetry stands out as the premier technique for electrochemical measurements, adeptly facilitating the characterization of electrochemical systems without necessitating specialized expertise. By monitoring how the current varies with potential, it allows for the elucidation of electrochemical properties through the analysis of current-potential (i-E) relationships. While faradaic and capacitive behaviors can be clearly described by straightforward equations, the characterization of constant phase elements (CPE) presents more complex challenges due to the absence of simple descriptive equations.

In this study, we developed a simplified approach for characterizing the CPE, focusing on the determination of the parameters n and Y_0, as delineated in Equations (6) and (7). Despite its advantages, this method still has a weak point. Specifically, while the n value can be determined with high precision, the estimation of Y_0 relies on numerical approximation, introducing potential for error. However, our findings across various experimental conditions confirm that these errors remain within a tolerable few percent, underscoring the method's reliability.

For more accurate characterization of CPEs, electrochemical impedance spectroscopy (EIS) remains the gold standard, albeit at the expense of increased measurement time. Given these

considerations, our alternative approach stands out as an expedient and reasonably accurate diagnostic tool, offering a balance between convenience and precision that is particularly valuable for preliminary assessments before more detailed and time-consuming analyses.

Acknowledgments:

This work was supported by a Research Grant of Pukyong National University(2023).

Scheme 1.

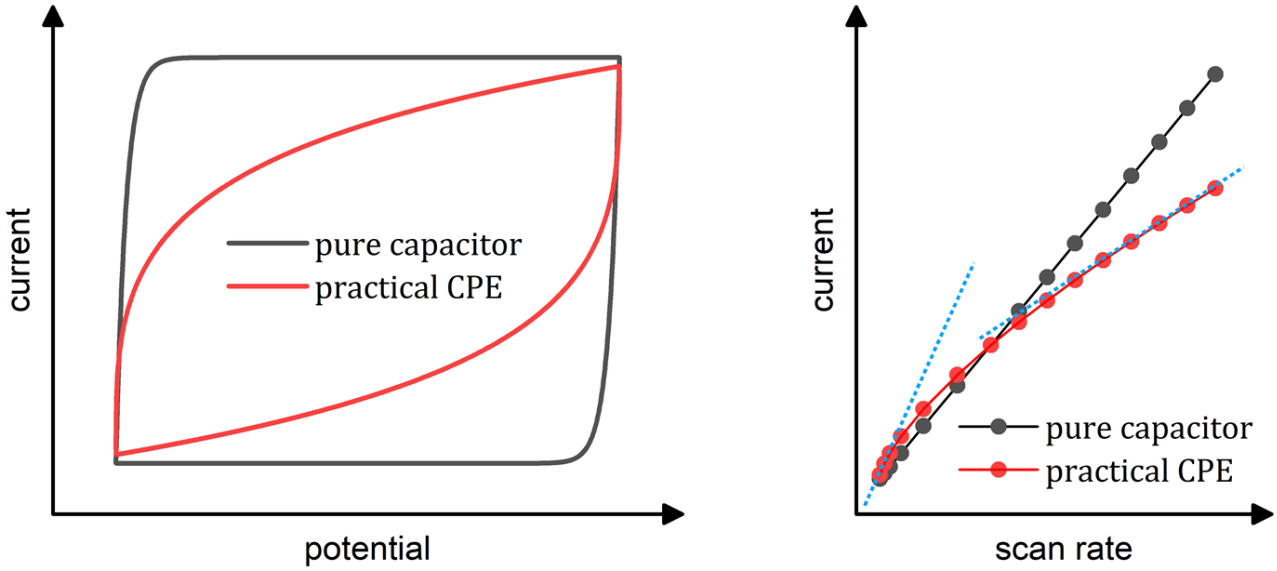

Figures:

Fig 1.

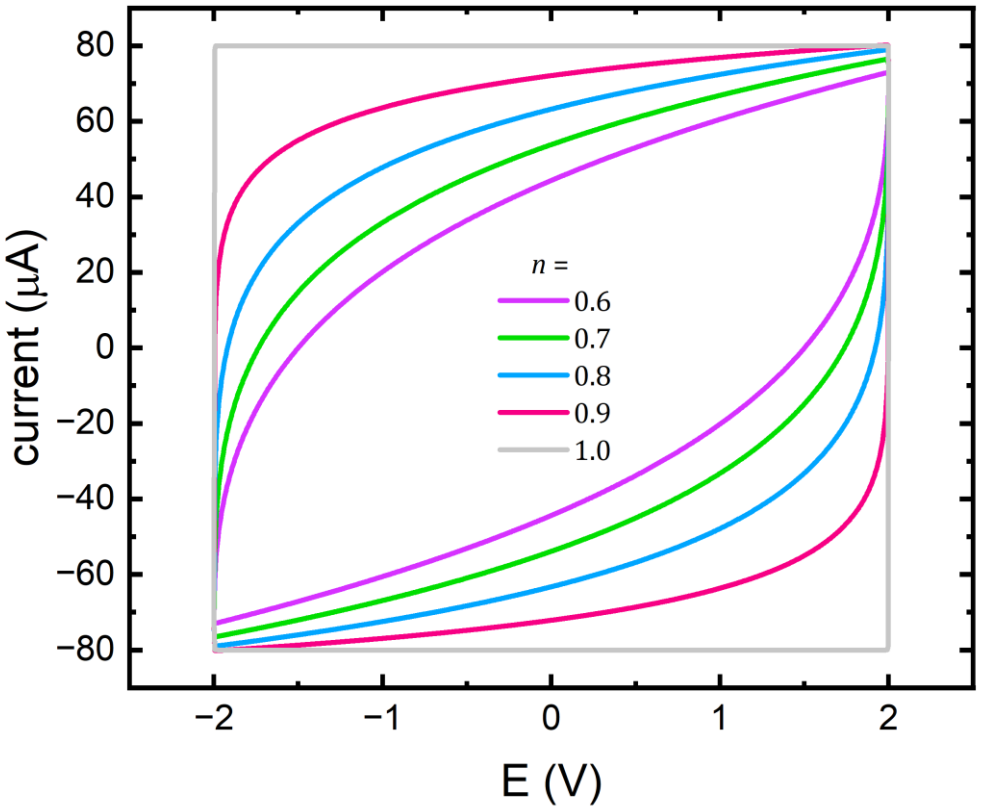

Fig 2.

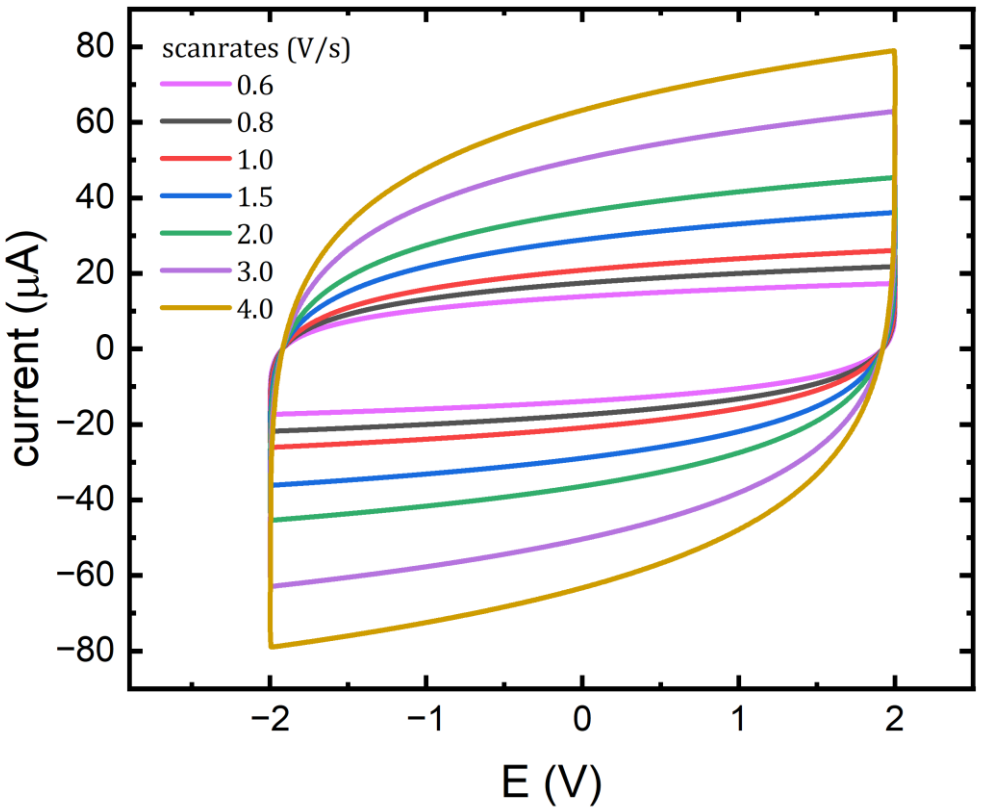

Fig 3.

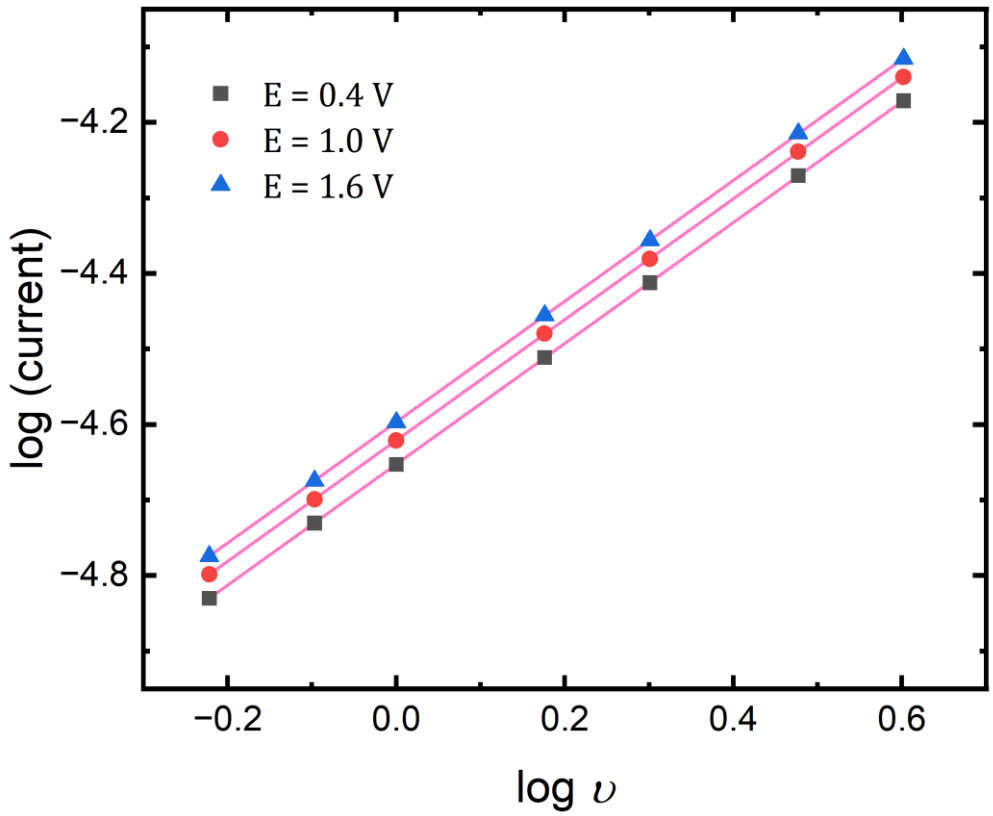

Fig 4.

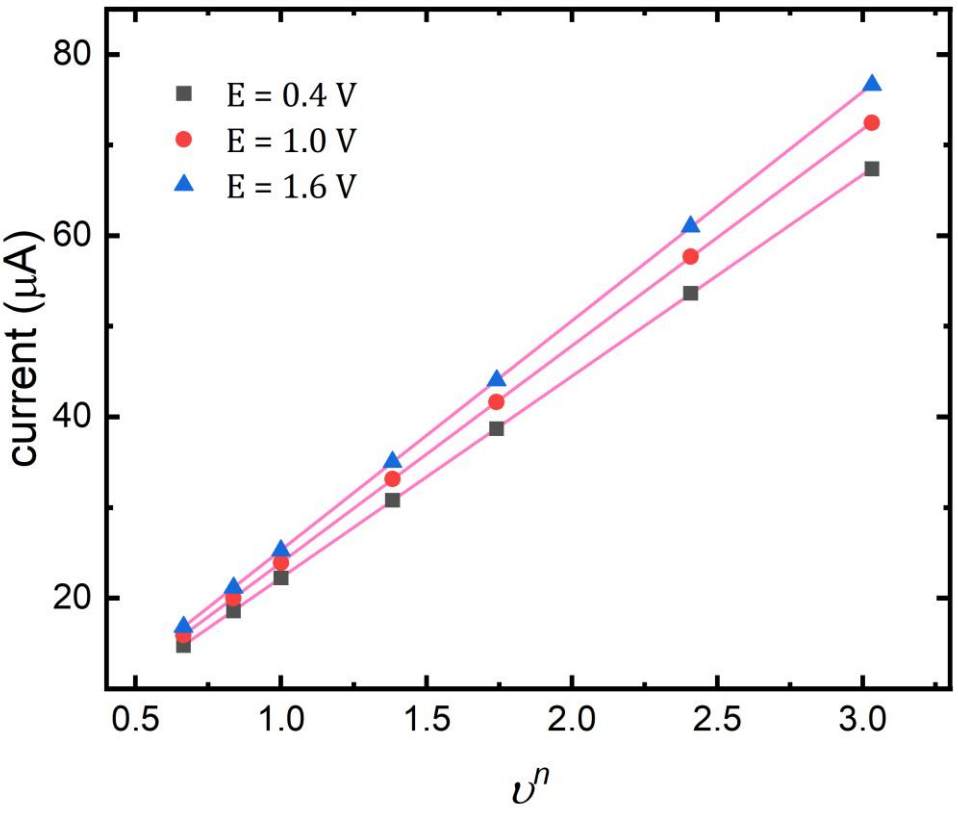

Fig 5.

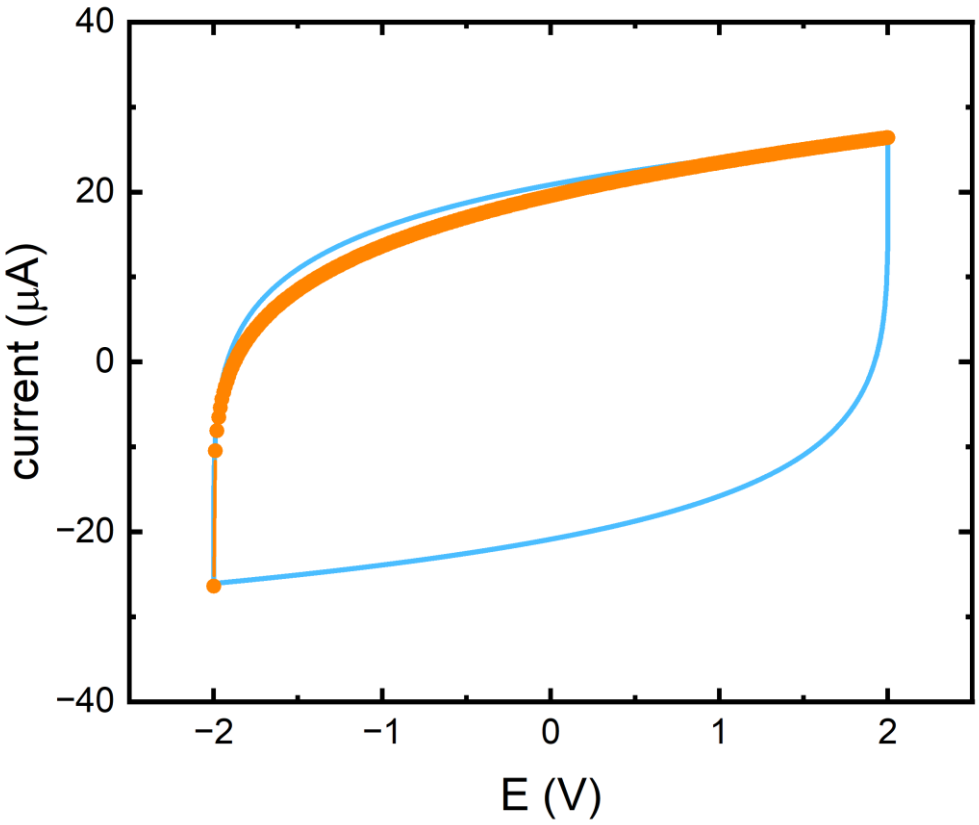

Fig 6.

(a)

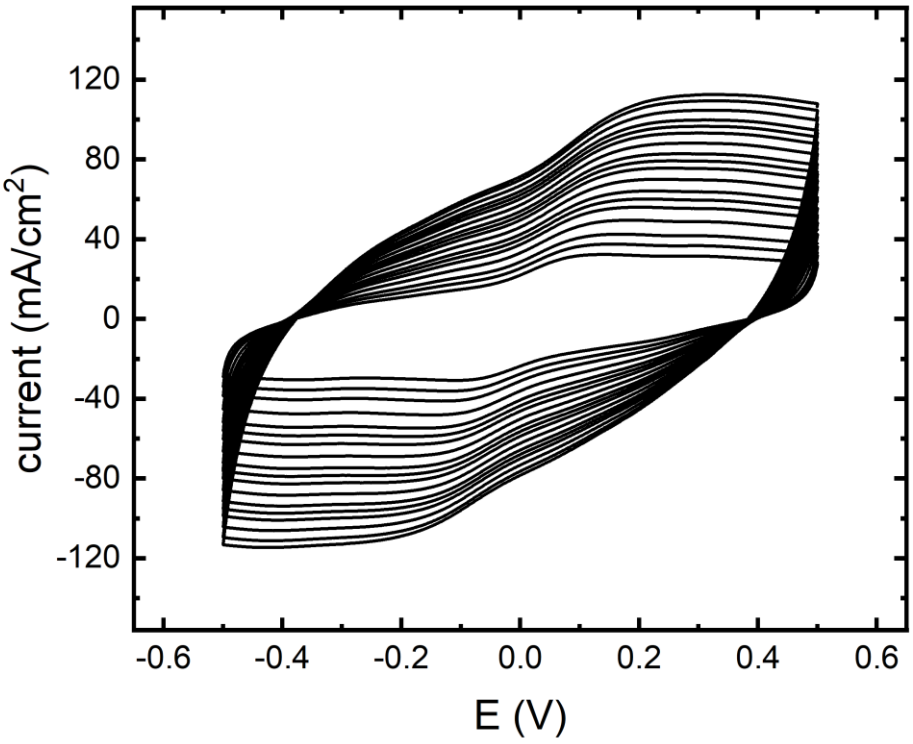

(b)

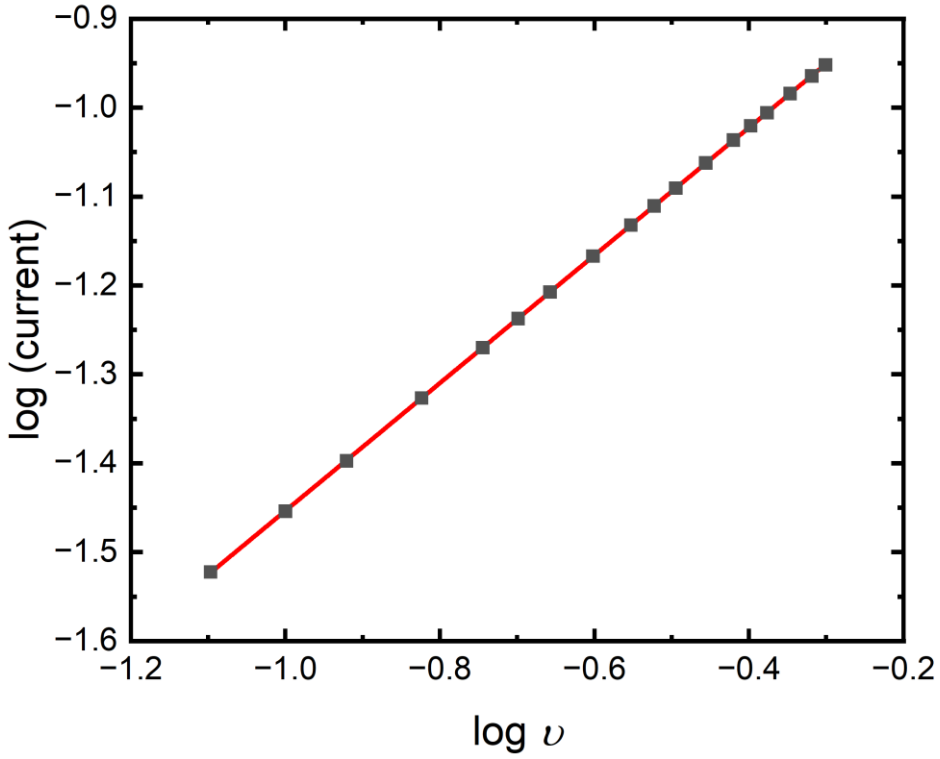
−0.9
−1.0
−1.1
−1.2
−1.3
−1.4
−1.5
−1.6
log (current)
−1.2
−1.0
−0.8
−0.6
−0.4
−0.2
log υ

Fig 7.

(a)

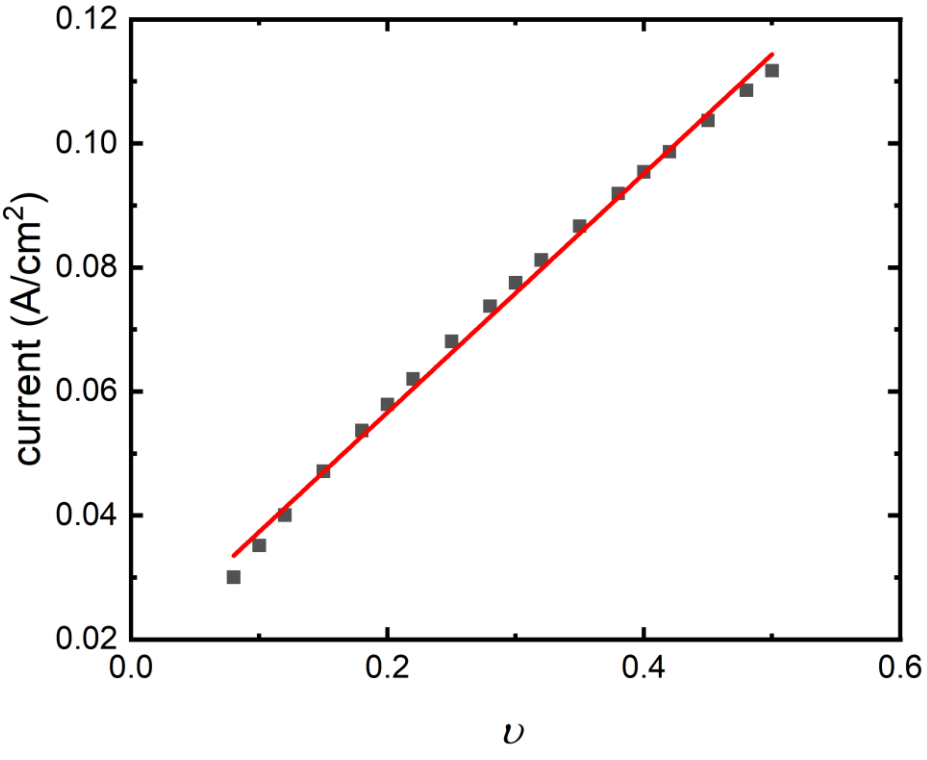
0.12
0.10
0.08
0.06
0.04
0.02
current (A/cm²)
0.0
0.2
0.4
0.6
υ

(b)

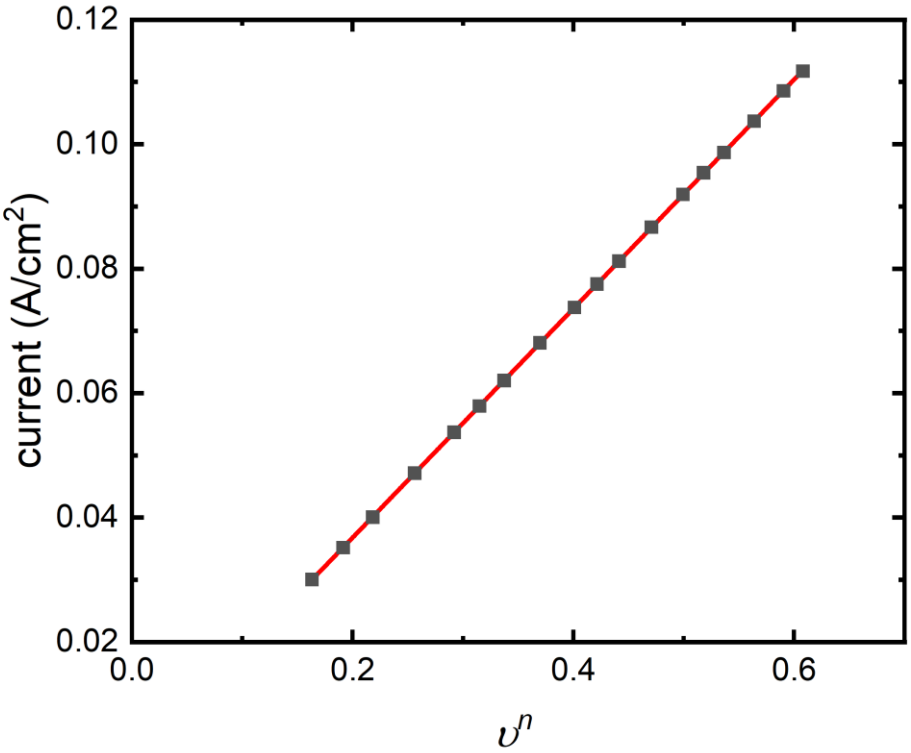

Fig 8.

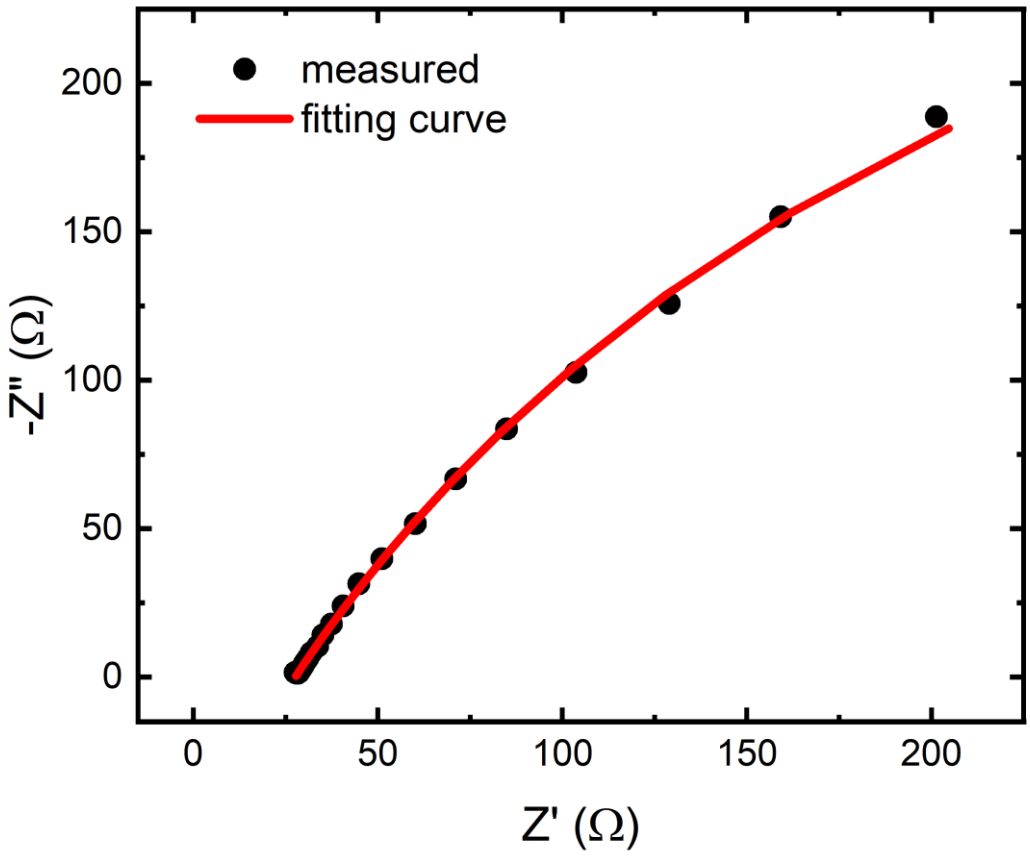

Fig 9.

(a)

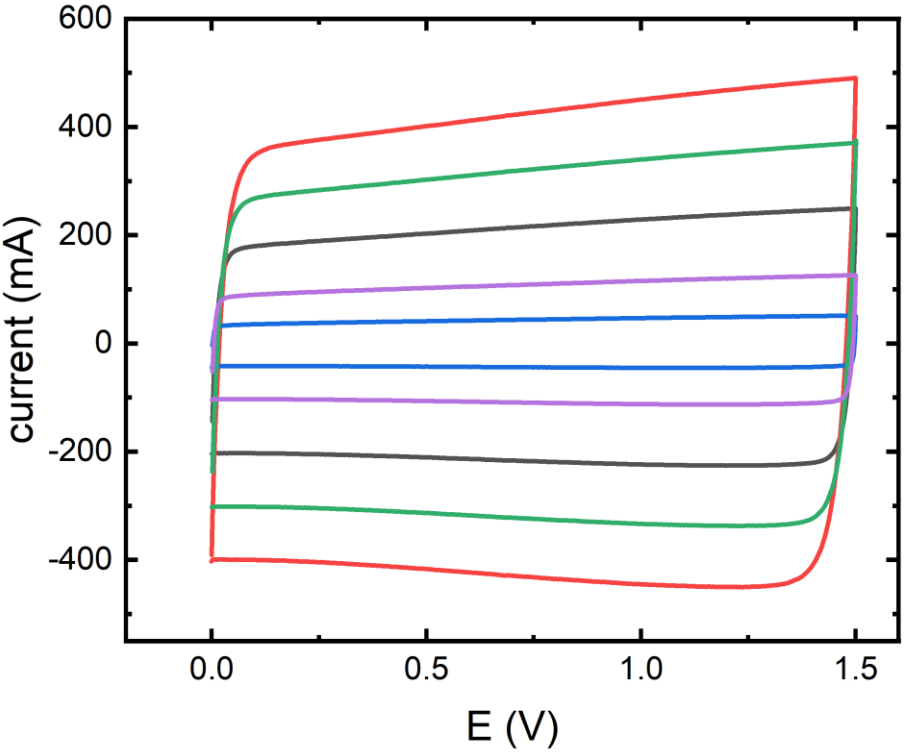

(b)

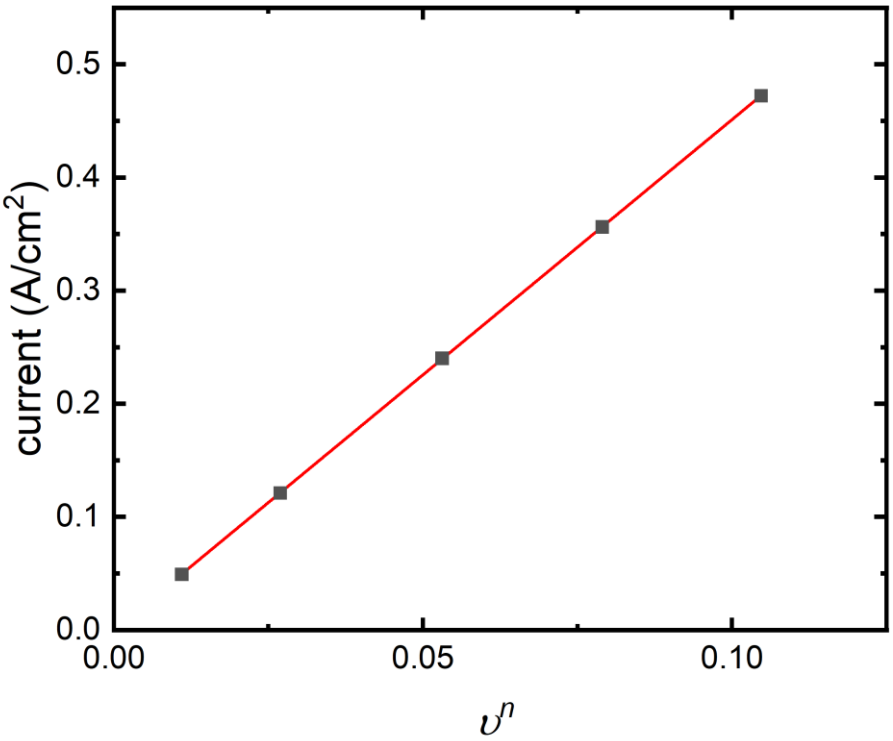

Table 1.

n \ ΔE	0.5	1.0	1.5	2.0	3.0	4.0
0.70	4.46	4.33	4.28	4.17	4.24	4.14
0.75	2.71	2.60	2.53	2.38	2.47	2.32
0.80	1.32	1.23	1.15	0.95	1.07	0.84
0.85	0.34	0.26	0.16	0.07	0.07	0.25
0.90	0.23	0.30	0.40	0.67	0.51	0.93
0.95	0.35	0.39	0.50	0.80	0.26	1.15
1.00	0	0.02	0.13	0.47	0.27	0.9

Captions:

Fig 1. Cyclic voltammograms for a constant phase element (CPE) across a range of *n* values (0.6, 0.7, 0.8, 0.9, and 1.0); $n = 1$ represents ideal capacitive behavior while *n*s deviated from 1 indicate non-ideal characteristics.

Fig 2. Cyclic voltammograms for a CPE with $n = 0.8$ across various scan rates, which demonstrates an increase in current response with increasing scan rates, albeit non-linearly. Such non-linear increases in current suggest the non-ideal capacitive behavior of the CPE.

Fig 3. Log-log plot of current vs. scan rate (v) for a CPE at selected potentials of 0.4 V, 1.0 V, and 1.6 V, demonstrating the linear relationship between log(current) and log v, which is consistent across different potentials, as expected from eq (5).

Fig 4. Plot of current (μA) against the scan rate raised to the power of n (v^n) for a CPE at $E = 0.4$ V, 1.0 V, and 1.6 V, showing a linear increase in current with v^n.

Fig 5. Comparison between the voltammograms obtained by eq (4) (orange curve) and computational simulation (blue curve). The orange curve is calculated on the assumption of a steady-state condition, and the blue curve is directly from the frequency domain function, eq. (2) by inverse Fourier transform.

Fig 6. (a) Cyclic voltammograms of a polyaniline pseudo-capacitor at various scan rates, and (b) the corresponding log-log plot of current *vs*. scan rate (v), confirming a linear relationship indicative of CPE behavior, with an n value obtained from the slope of the fitted line.

Fig 7. Plots of the currents *vs*. v in (a) and v^n in (b) for the polyaniline pseudo-capacitor. The current linearly increase with v^n which indicates that the system is more accurately modelled with a CPE rather than a capacitor where the linear slope is used to estimate the Y_0 value of the CPE.

Fig 8. Nyquist plot of the EIS data for a polyaniline pseudo-capacitor, showing measured impedance (black dots). The data are fitted to an equivalent circuit contains a CPE to evaluate the values of n and Y_0 with the fitting curve (red line).

Fig 9. (a) Cyclic voltammograms of a commercial supercapacitor at various scan rates demonstrating non-ideal capacitive behavior, and (b) a linear plot of the current *vs.* v^n, illustrating the linear correlation indicative of the CPE model. The slope of the linear fit is used to calculate the Y_0 value, consistent with the specified capacitance of the supercapacitor.

Table 1. Relative errors (%) in the estimation of the Y_0 values of across ranges of n and potential windows (ΔE) using eq (7).

References:

[1] Bard, A. J.; Zoski, C. G. *Anal. Chem.* **2000**, *72*(9), 346 A-352 A.

[2] Elgrishi, N.; Rountree, K. J.; McCarthy, B. D.; Rountree, E. S.; Eisenhart, T. T.; Dempsey, J. L. *J. Chem. Educ.* **2018**, *95*(2), 197-206.

[3] Rafiee, M.; Abrams, D. J.; Cardinale, L.; Goss, Z.; Romero-Arenas, A.; Stahl, S. S. *Chem. Soc. Rev.* **2024**, *53*(2), 566-585.

[4] González, J.; Laborda, E.; Molina, Á. *J. Chem. Educ.* **2023**, *100*(2), 697-706.

[5] Kim, B.-K.; Park, K. *J. Electrochem. Sci. Technol.* **2022**, *13*(3), 347-353.

[6] Scholz, F. *ChemTexts* **2015**, *1*(4), 17.

[7] Sandford, C.; Edwards, M. A.; Klunder, K. J.; Hickey, D. P.; Li, M.; Barman, K.; Sigman, M. S.; White, H. S.; Minteer, S. D. *Chem. Sci.* **2019**, *10*(26), 6404-6422.

[8] Huang, X.; Wang, Z.; Knibbe, R.; Luo, B.; Ahad, S. A.; Sun, D.; Wang, L. *Energy Technol.* **2019**, *7*(8), 1801001.

[9] Aderyani, S.; Flouda, P.; Shah, S. A.; Green, M. J.; Lutkenhaus, J. L.; Ardebili, H. *Electrochim. Acta* **2021**, *390*, 138822.

[10] Wang, H.; Pilon, L. *Electrochim. Acta* **2012**, *64*, 130-139.

[11] Bhojane, P. *J. Energy Storage* **2022**, *45*, 103654.

[12] Lasia, A. *J. Phys. Chem. Lett.* **2022**, *13*(2), 580-589.

[13] Chang, B.-Y.; Park, S.-M. *Annu. Rev. Anal. Chem.* **2010**, *3*(1), 207-229.

[14] Vivier, V.; Orazem, M. E. *Chem. Rev.* **2022**, *122*(12), 11131-11168.

[15] Córdoba-Torres, P.; Mesquita, T. J.; Nogueira, R. P. *J. Phys. Chem. C* **2015**, *119*(8), 4136-4147.

[16] Douglass Jr, E. F.; Driscoll, P. F.; Liu, D.; Burnham, N. A.; Lambert, C. R.; McGimpsey, W. G. *Anal. Chem.* **2008**, *80*(20), 7670-7677.

[17] Chang, B.-Y. *J. Electrochem. Sci. Technol* **2022**, *13*(4), 479-485.

[18] Bograchev, D. A.; Volfkovich, Y. M.; Martemianov, S. *J. Electroanal. Chem.* **2023**, *935*, 117322.

[19] Chang, B.-Y. *Electrochim. Acta* **2023**, *462*, 142741.

[20] Sadkowski, A. *Electrochim. Acta* **1993**, *38*(14), 2051-2054.

[21] Sagüés, A. A.; Kranc, S. C.; Moreno, E. I. *Corros. Sci.* **1995**, *37*(7), 1097-1113.

[22] Feliu, V.; González, J. A.; Feliu, S. *Corros. Sci.* **2007**, *49*(8), 3241-3255.

[23] Zheng, J. P.; Pettit, C. M.; Goonetilleke, P. C.; Zenger, G. M.; Roy, D. *Talanta* **2009**, *78*(3), 1056-1062.

[24] Zheng, J. P.; Goonetilleke, P. C.; Pettit, C. M.; Roy, D. *Talanta* **2010**, *81*(3), 1045-1055.

[25] Allagui, A.; Freeborn, T. J.; Elwakil, A. S.; Maundy, B. J. *Sci. Rep.* **2016**, *6*(1), 38568.

[26] Charoen-amornkitt, P.; Suzuki, T.; Tsushima, S. *Electrochim. Acta* **2017**, *258*, 433-441.

[27] Charoen-Amornkitt, P.; Suzuki, T.; Tsushima, S. *Electrochemistry* **2019**, *87*(4), 204-213.

[28] Charoen-Amornkitt, P.; Suzuki, T.; Tsushima, S. *J. Electrochem. Soc.* **2020**, *167*(16), 166506.

[29] Yun, C.; Hwang, S. *ACS Omega* **2021**, *6*(1), 367-373.

[30] Schalenbach, M.; Durmus, Y. E.; Tempel, H.; Kungl, H.; Eichel, R.-A. *Phys. Chem. Chem. Phys.* **2021**, *23*(37), 21097-21105.

[31] Gateman, S. M.; Gharbi, O.; Gomes de Melo, H.; Ngo, K.; Turmine, M.; Vivier, V. *Curr. Opin. Electrochem.* **2022**, *36*, 101133.

[32] Costentin, C. *J. Phys. Chem. Lett.* **2020**, *11*(22), 9846-9849.

[33] Hong, S.-Y.; Park, S.-M. *J. Phys. Chem. B* **2007**, *111*(33), 9779-9786.